Chapter 2

Synthesis and characterization techniques

2.1 Overview

This chapter provides a brief description of the synthesis/growth methods used to produce the studied compounds/single crystals, followed by an overview of the experimental techniques that have been utilised to characterise them in this thesis. All the $NiBr_2$ samples investigated in this thesis were single crystals that were provided by Dr. Yingkai Huang in collaboration with the University of Amsterdam and were grown using the self-flux growth approach. The traditional solid-state synthesis process was adopted to produce polycrystalline Mn-doped $SmFeO_3$ (SFMO) and Cd-doped Cu_2 $OSeO_3$ (CSO) samples. Single-crystals of SFMO were grown using a four-mirror optical float-zone furnace (OFZF). In the second part, several macroscopic and microscopic methods are briefly reviewed. These techniques have been used to extract the structural, morphological, compositional, magnetic, and element-specific properties by employing various experimental techniques. For completeness, this section will provide references to previous works where the techniques are described in more detail when in-depth knowledge is required.

2.2 Synthesis/Growth method

The synthesis of high-quality powder samples (single-phase and presence of all elemental compositions in stoichiometric ratios) plays a vital role in obtaining excellent quality of a single crystal and the desired physical properties [96]. Hence, the selection of the sample

preparation method and heat treatment plays a key role in obtaining good quality seed and feed rods for single crystal growth along with careful handling of the intermediate steps. High-purity precursors should be used to avoid defects and contamination in the phase quality of the obtained compound. Along with a single-phase with proper elemental compositions, the synthesis conditions are also equally significant. During the synthesis process, parameters such as pressure, temperature, and reaction time need to be varied in accordance with the requirements of the sample. Generally, a solid-state reaction route or ceramic method is preferred to synthesize seed and feed rods in oxide materials for bulk single crystals using the optical floating zone technique.

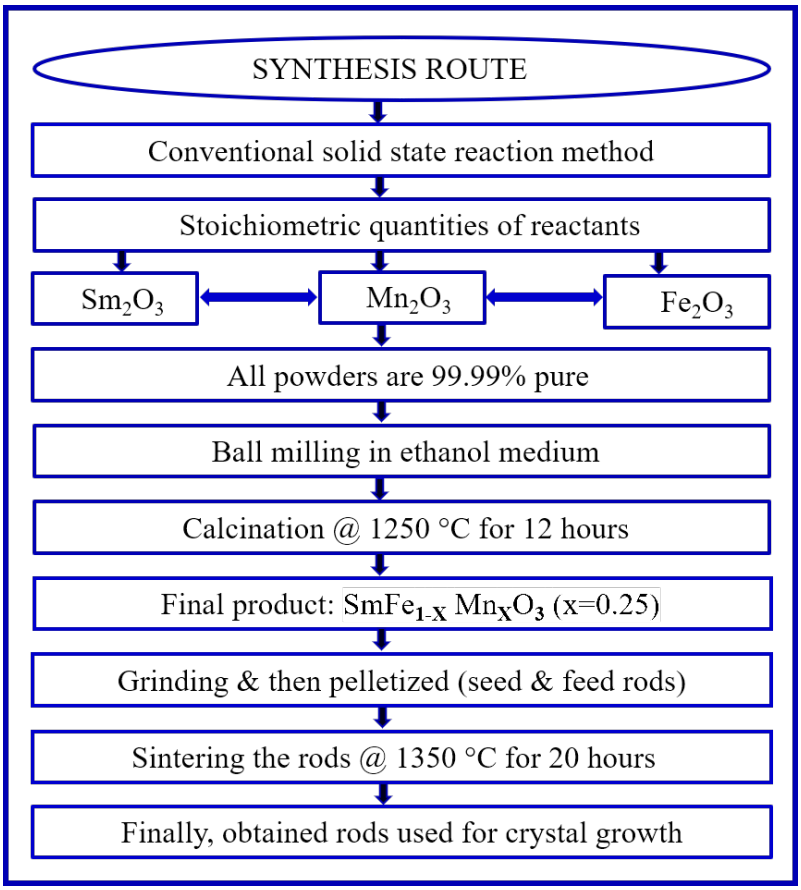

Fig. 2.1 Flow chart representation of sample preparation by conventional solid-state reaction route.

2.2.1 Solid-state reaction route

The solid-state reaction route has proven to be a versatile technique for complex oxide synthesis [97]. The SFMO and CSO powder samples were synthesised using a conventional solid-state reaction technique. The following steps in this study were adopted for the

synthesis of powder samples by a solid-state reaction route, which is described below in a flow chart (see Fig. 2.1) and details are given in itemize format [96].

• **Raw materials:** All starting materials are of high-purity powders of oxides. Powders are weighed to obtain the stoichiometric compositions of the resultant product.

• **Sample preparation:** In the solid-state reaction method, it is essential to mix and grind the powders thoroughly for a longer duration to obtain homogeneous distribution for the reaction to take place homogeneously. The proper grinding of mixed powders using a planetary ball mill reduces the particle size as much as possible up to a few nanometers, depending on various parameters such as milling time, speed, milling medium, size of balls, and weight of balls contained in jars. The rotation speed of 300 rpm, with an average weight of balls is 100 g milling for 15 hours were taken into consideration.

• **Ball milling:** Ball milling is a mechanical grinding technique widely used to blend and grind bulk materials into nanosized particles [98]. It consists of a hollow cylindrical container rotating around its axis, partially filled with stainless steel or ceramic balls. During the ball milling process, the energy released from the impact and attrition between the balls, that is, grinding or milling medium, and the powder in a concealed container results in attrition size reduction. The advantages of this technique include cost-effectiveness, ease of operation, reliability, reproducibility due to energy and controlled speed, and applicability in dry and wet conditions on a broad range of materials. In contrast, the major disadvantages include the possibility of contamination, nanomaterial formation with an irregular shape, and cleaning times.

After ball milling, the obtained powder mixture was heated in an air atmosphere for the first time. This first calcination process helps to remove the volatile species present in the mixture. After the first heating, further heating in the air is required to obtain phase purity and remove any traces of volatile species present, if any. It is always better to increase the temperature gradually during the heat treatment process to avoid the deficiency of O_2 in oxide materials.

• **Sintering:** The obtained adequate black calcined powder sample is pressed into cylindrical rods shape (see Fig. 2.2) to obtain feed and seed rods for single crystal growth. The rods were sintered in an air furnace at a temperature of 1350 °C for 20 h to obtain high-density rods. The samples were allowed to cool very slowly in a furnace; this process is called sintering, as shown in Fig. 2.1.

Finally, the obtained sintered feed and seed rods were used for single crystal growth.

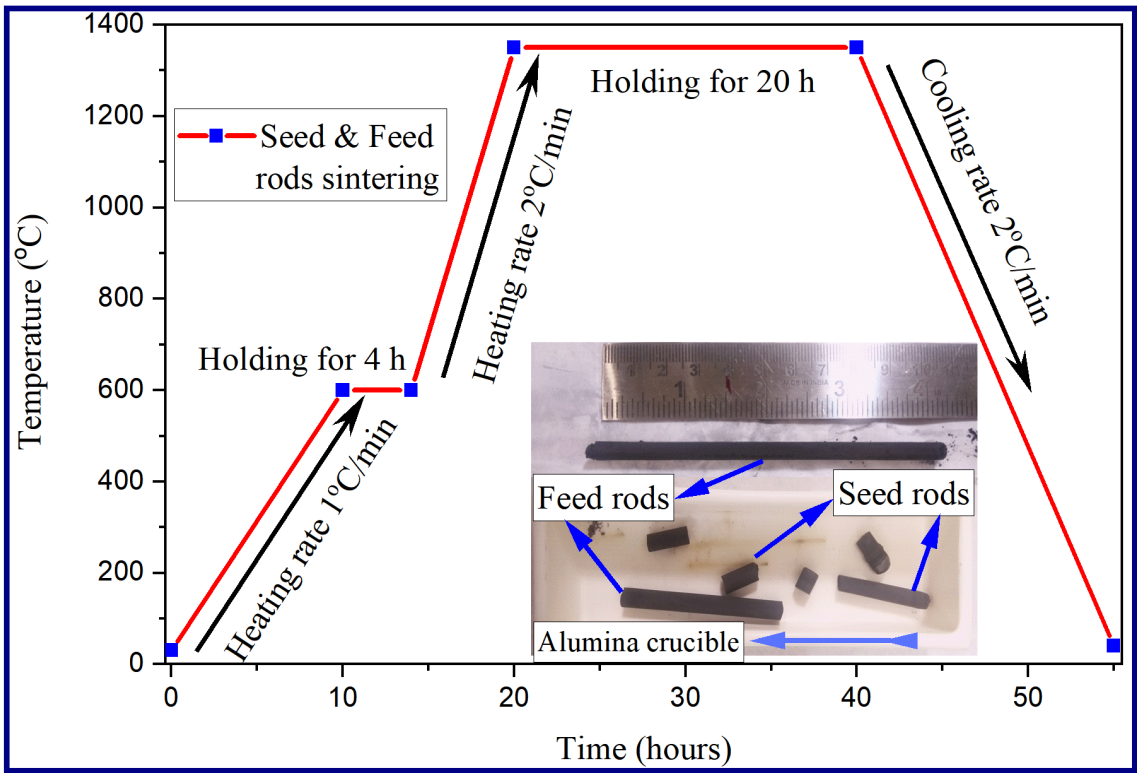

Fig. 2.2 Temperature versus time graph of reactive sintering process.

2.2.2 Optical floating zone technique

The floating zone technique is a purification strategy involved in crystal growth, where a narrow region of the feed rod melted in which impure solids are also melted. The present impurities move in an upward direction of the molten zone, and pure materials move towards the seed rod. This process is called zone refining, zone melting, or floating zone processes [99].

The optical floating zone (OFZ) technique is an excellent method for growing large pieces of single crystals of complex oxide materials with a high melting temperature. In this technique, limitations exist in growing metallic samples that have high reflectivity but are highly useful for growing oxides and semiconductor materials. The melting zone is formed at the focal point of the ellipsoidal mirrors with the help of spontaneous radiation from halogen or xenon lamps of a wide range of power to form a better-molten zone, which translated perpendicular to the crystal growth direction, as shown in Fig. 2.3. Initially, the optical float zone furnace (image furnace) was designed with one or two mirrors, later upgraded to a system having four mirrors, and was found to have a compact design [100].

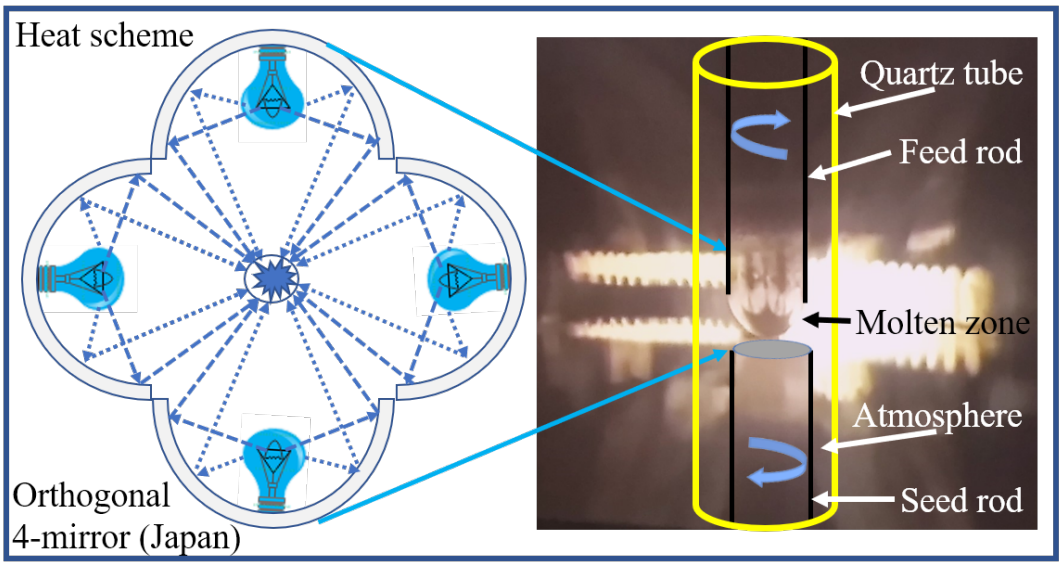

Fig. 2.3 Principle of four mirror optical floating zone (OFZ) method.

In contrast to other mirror setups, four mirrors provide uniform point heating, reduce the temperature gradient in the growing crystal, and suppress the thermal stress of the grown crystal. The optimisation of various growth parameters is required to obtain a stable molten zone yielding a quality single crystal. The material properties to care for are viscosity, melting point, phase diagram, density, purity, which can affect the crystal dimension and floating zone [99]. An algorithmic representation of the growth process is presented in Fig. 2.4. The various growth parameters that one has to take care of during the growth of a single crystal are feed rod, seed rod, growth rate, rotation rate, atmosphere, gas pressure, temperature gradient, molten zone, and power. The details of these parameters are described in detail below.

• **Feed rod:** In the OFZ furnace, the feed rod plays a vital role in growing an excellent quality of a large single crystal. Feed rods were made with a solid solution by pressing in dye at 70 MPa pressure, fulfilling the requirements for producing high-quality crystals. The requirements are single-phase, highly dense feed rod, straight, uniform diameter, homogeneous in the composition used to maintain a stable molten zone dimension. The highly porous feed rod disturbs crystal growth by initiating incongruent melting. A pictorial representation of the feed rod is presented in Fig. 2.5 (a). Therefore, it is necessary to reduce the porosity of the rod by optimising the sintering temperature before assembling it in the image furnace. Here, the optimised sintering temperature was 1350 °C, near the

melting point of the compound. The effect of porosity during the growth process is well known for incongruent melting [101].

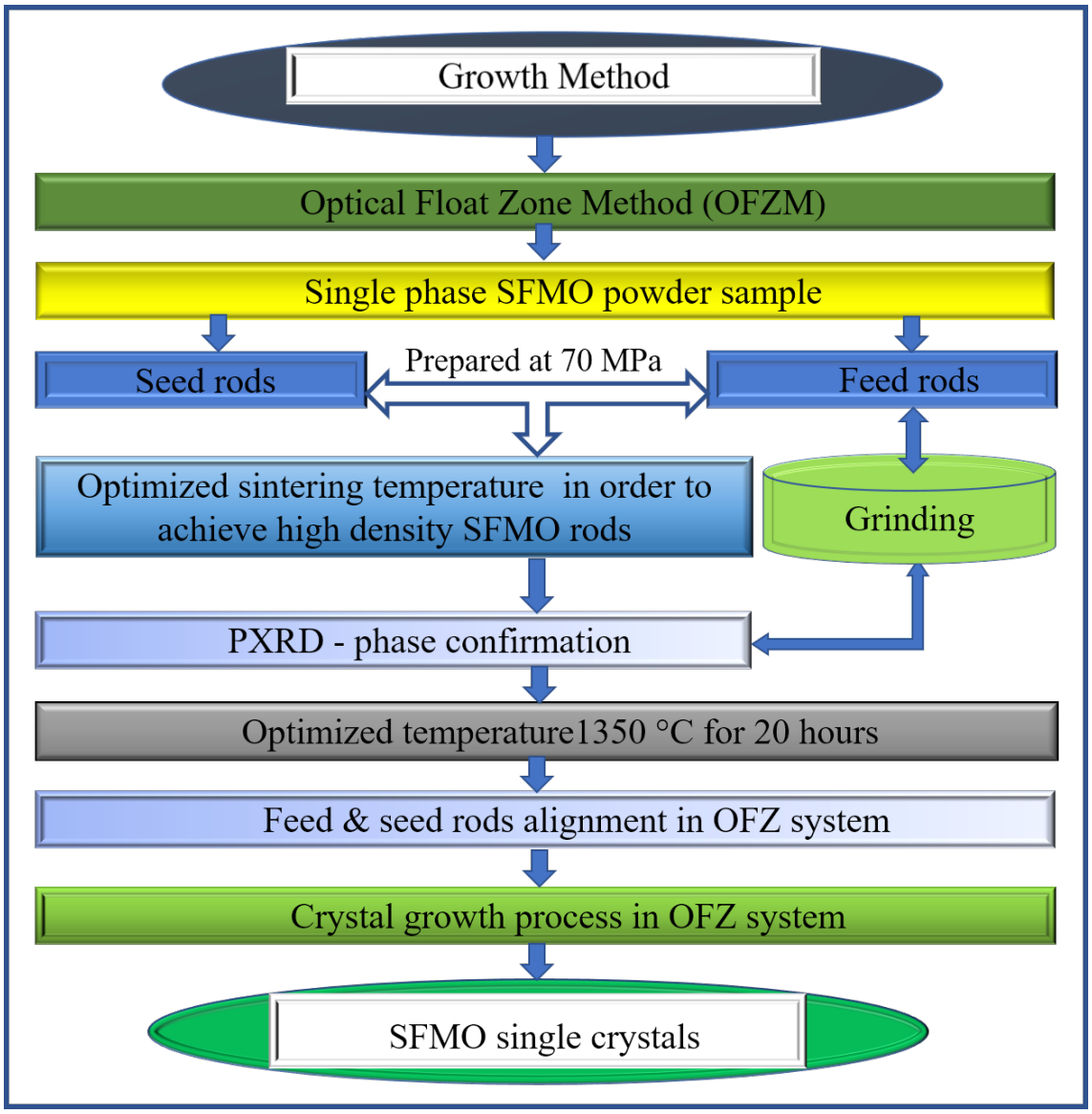

Fig. 2.4 Flow chart representation of single crystal growth by OFZ technique.

• **Seed rod:** The seed rods are also prepared by the same process as feed rods or using an orientated or unoriented crystal as a seed rod. In this technique, the seed should be tightly packed in the seed holder. The seed rods used in the OFZ method are shown in Fig. 2.5(b) at the bottom.

• **Rotation rate:** The regulation of the rotation rate of feed & seed rods plays an important role in homogeneous mixing of the molten zone and shaping the crystal by

controlling the convection force. This technique can rotate the feed and seed rods independently in the counterclockwise direction. Higher rotation rates lead to a high convection force, which transports the heat absorbed on the melt surface, lowering the convexity of the interface results in a uniformly shaped crystal. The stable molten zone enhances the morphological stability of the crystal, and the rate of rotation obtained for the stabilised molten zone does not affect the growth process but can affect the molten zone during the growth mechanism [101, 102]

• **Growth rate:** Translation rate or growth rate is an important parameter in the crystal growth method, it may affect the crystals nature, size, defects, changing in the growth direction, changing crystal position, bubbles, molten zone stability, and leading to the formation of secondary phases. In general, the growth rate levied on material characteristics, whether materials belong to a congruent or incongruent melting nature. If the molten zone melts congruently, the growth rate will be relatively higher, and if it is incongruently melted due to variation in the melting point of the multiple-component system, the growth rate is low, which is governed by the compositional variation [101]. From the reported experimental data, high-quality crystals with a large size were obtained from a lower growth rate and prevented defects. A higher growth rate induces thermal stress, inhomogeneity, defects, and reduces the material strength to form hairline cracks in the grown single crystals. A lower growth rate suppresses the characteristics, but material characteristics require a faster growth rate to obtain defect-free single crystals in some cases. The materials with a decomposition point are very close to the melting point, which requires a faster growth rate. The optimised growth rate shows a spiral pattern in surface morphology, indicating a defect-free single-crystal [103].

• **Growth pressure and atmospheric medium:** Atmosphere medium and pressure are two different parameters that influence the growth of high-quality single crystals by the OFZ technique. Careful selection of atmospheres such as air, oxygen, argon, vacuum, nitrogen, and other gases are required to control the deficiency of compositions, inhomogeneity, and bubbles in the molten zone. Generally, an oxygen medium is preferred for oxide materials to avoid oxygen vacancies or excess oxygen in the grown crystal. For metals, a vacuum or argon atmosphere is preferred to prevent oxidation at higher temperatures. Most of the crystals are grown in an air atmosphere except in a few exceptional cases; the used rare-earth orthoferrite crystals are grown in an air atmosphere. The gas pressure increases the melting point of the compound in various atmospheres, so a high lamp power is required for melting. However, it is important to reduce the vaporisation of volatile materials during growth. The main advantage of growing crystals at high pressure is their

homogeneity. By controlling parameters such as pressure and atmosphere, it restricts the secondary phase and yields high-quality single crystals [103, 104].

2.2.3 Mn-doped samarium ortho-ferrite (Mn-$SmFeO_3$) crystal growth:

Single crystals of SFMO were grown in a four-mirror optical float-zone furnace (OFZF) (Crystal System Ins., model FZ-T-10000-H-HR-I-VPM-PC) using four 1 kW halogen lamps at the IISER Pune. The proper assembly of seed and feed rods plays an important role in controlling the growth process in the OFZF method. Fig. 2.5 (b) shows the seed and feed rods assembled in the optical furnace, and the background of Fig. 2.5 shows the image of four optical lamps. The feed rod was aligned at the centre, nearly above 2 mm the focal point, and the seed rod assembled at the centre was nearly 10 mm below the focal point. Improper alignment of the seed and feed rod leads to instability in the growth of high-quality single crystals. The seed and feed rod were mounted at the centre and rotated simultaneously in the opposite direction. The complete system was then sealed. The temperature of the molten zone was carefully controlled by adjusting the power of the lamps. At a critical power of 64.5 % of 1000 W × 4 was used to start the crystal growth process as 2.5 (c) in air medium. During the growth process, as shown in Fig. 2.5 (d), the molten zone moved upwards at a rate of 3-6 mm h^{-1}, with the seed rod and feed rod in sample holder stages called as lower shaft and upper shaft, respectively. Both are counter-rotating at 20 rpm in an airflow of 0.2 L min^{-1} [105]. During crystal growth,

Table 2.1 Variation of growth parameters during single crystal growth

Time (IST)	Uper shaft speed (mm/hr)	Lowe shaft speed (mm/hr)	Uper shaft rotation (rpm)	Lower shaft rotation (rpm)	Uper shaft move (mm)	Air flow rate (lt/mint.)	Growth lenght (mm)	Power (%)
10.00	0.00	1.00	9.40	9.20	0.00	1.00	0.00	36.01
10.30	0.00	1.00	9.40	9.20	0.50	1.00	0.00	62.00
@Power 64% (Lamp power: 1000 Watt X 4), start melting								
14.00	5.00	5.00	20.00	20.00	3.50	0.20	0.40	64.50
15.00	5.00	5.00	20.00	20.00	8.40	0.20	5.40	64.50
16.00	5.00	5.00	20.00	20.00	12.70	0.20	9.60	64.50
17.00	5.00	5.00	20.00	20.00	17.90	0.20	14.7	64.50
Float zone start narrowing, and becomes disconnected. The lower shaft stop and upper shaft continue to move. The power increased to 65.1%, again joined.								
17.30	5.00	5.00	20.00	20.00	18.00	0.20	15.00	64.40
18.00	5.00	5.00	20.90	18.20	21.00	0.20	17.90	64.40
Zone was going down, and broken, Again joined by adjusting various parameters like movement of upper and lower shaft and power.								
19.00	4.90	5.20	21.9	19.10	29.20	0.20	22.50	64.40

the various optimised growth parameters are listed in Table 2.1. After crystal growth, the as-grown single crystal is shown in Fig. 2.5 (e), and a photograph of the (a-b) disk after cutting with a diamond cutter and alignment with a Laue diffractometer is shown in Fig. 2.5 (f).

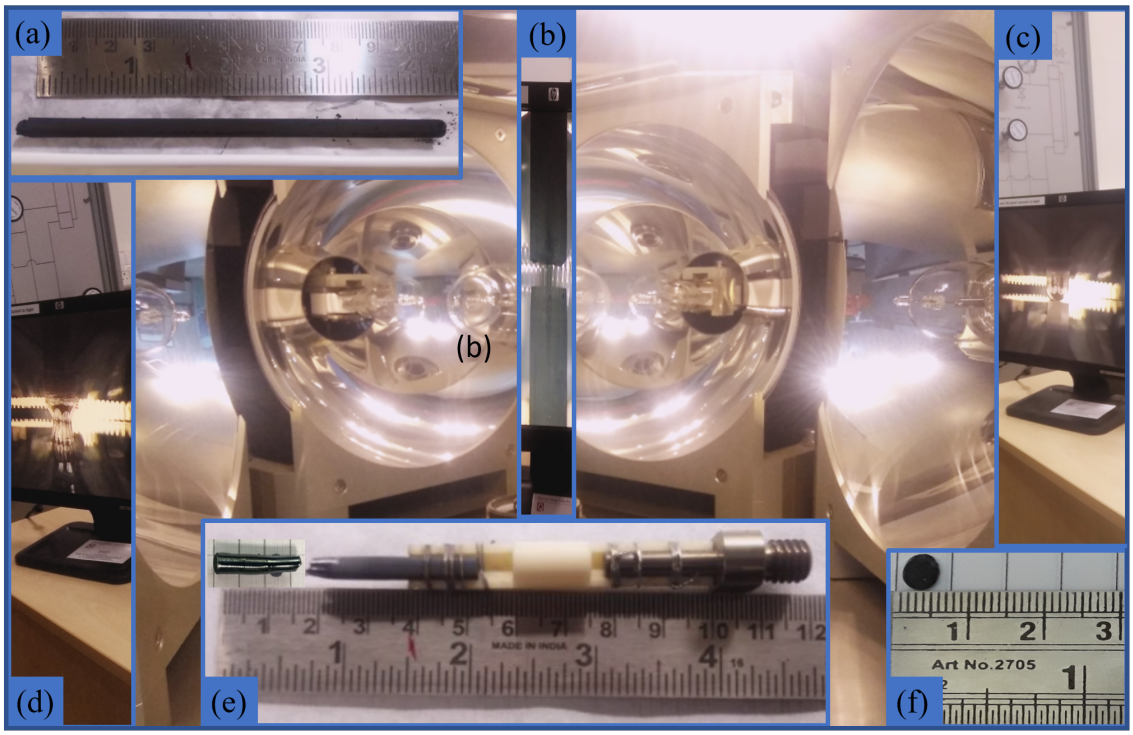

Fig. 2.5 SFMO single crystal growth process (a) photo of seed rod, (b) seed rod on sample holder stages, (c) starting of crystal growth, (d) during crystal growth, (e) after crystal growth, as-grown single crystal, and (f) photo of (a-b) disk after cutting and alignment.

2.3 Characterization techniques & working principle

Understanding the scientific and technological benefits of grown single crystals is impossible unless their characterisation is made. The process of understanding their properties, compositions, morphology, crystal, and magnetic structure is called characterisation, which plays an important role in identifying the physical and chemical properties of a material and is essential for the proper implementation of substances when used in scientific applications or industries (see Fig. 2.6) [106]. In this section, briefly present the characterisation techniques employed in this thesis: X-ray diffraction, Laue diffraction for single crystals, transmission electron microscopy (TEM), scanning electron microscopy (SEM), energy dispersive X-ray analysis (EDX), ac magnetisation, dc susceptibility, and small-angle neutron scattering (SANS).

2.3.1 X-ray diffraction

The most common tool for phase confirmation of polycrystalline materials is powder X-ray diffraction (XRD or PXRD), which produces a characteristic diffraction pattern fingerprint

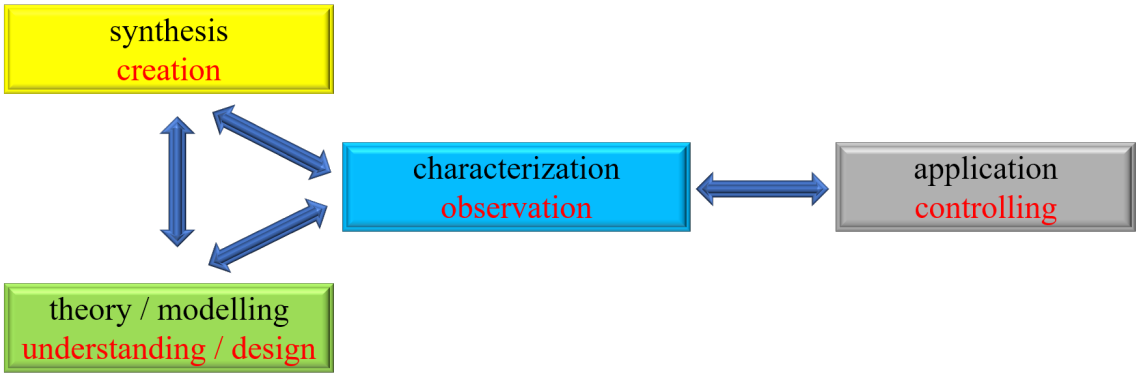

Fig. 2.6 Characterization is the nexus between synthesis, realization, and application of magnetic materials and underlying spin structures.

that widely used for phase confirmation and or identification. XRD is one of the most versatile methodologies, suitable for bulk materials (solid-solution) as well as for thin films to study the crystal structure, phase, and other structural parameters, such as average grain size, strain, crystallinity, and crystal defects. As the physical properties of solids highly depends on atomic arrangements of materials, the determination of the crystal structure is a major part of the materials characterization. X-rays are used to measure the diffraction pattern as their wavelength (λ) in a typical range of (1-100 Å) as the inter-planer spacing, d between the planes in the crystal system lies in the same range. Therefore, the interference of coherently scattered radiation in these materials will form a diffraction pattern. For the detailed description and the theory of diffraction, which is well established and the experimental setup of a modern laboratory diffractometer is described in many textbooks, see the references [107–110].

The structural properties and crystalline phases of the grown crystals were analysed by X-ray diffraction (XRD). In this study, the X-ray patterns of all the samples were collected from 10° to 90° with a step size of 0.02°/s using an X-ray diffractometer (Rigaku Corporation, Tokyo, Japan) with monochromatic $\lambda_{K\alpha}^{Cu}$ = 1.54056 Å.

The powder sample consists of the various lattice planes that are present in every possible orientation with an inter-plane distance of d. Thus, a convergent monothematic X-ray beam is focused on a powder sample, which is diffracted in cones like pattern of radiation, the pattern is determined by the internal architecture of the powder sample, see Fig. 2.7. Taking the case of elastic scattering, the intensity will appear maximum for the scattering directions, results from the addition of the magnitude of moment of the incident particle and a vector belonging to the reciprocal lattice of the polycrystalline.

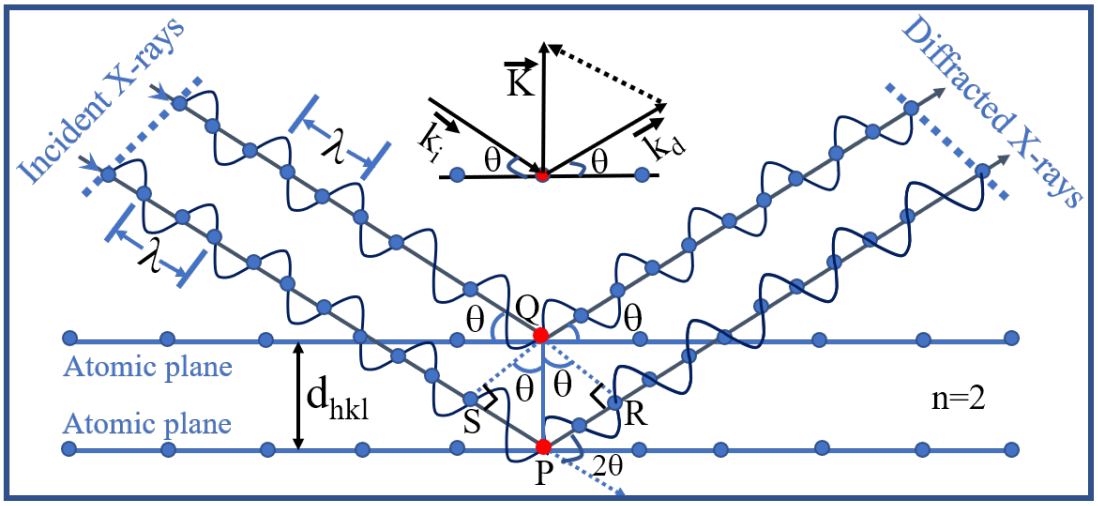

Fig. 2.7 Working principle of X-ray diffraction.

These directions are known as Bragg peaks or Bragg positions, and a set of Miller indices can be allotted to them.

The diffraction measurements provide the information in the reciprocal lattice, and therefore the real space lattice can be obtained as the Fourier transform of the reciprocal space. Each peak position satisfies Bragg's law:

$$n\lambda = 2d_{(hkl)}\sin(\theta) \tag{2.1}$$

where λ is the wavelength of the incident X-ray, d_{hkl} is the interplanar spacing between the planes with (hkl) Miller indexes, and 2θ is the angle of incidence formed by the propagation vectors of the scattered and incident X-rays. Diffraction data usually represented as the number of diffracted particle counts versus 2θ. Bragg's law (see Eq. (2.1)) can be used to calculate d-spacing to each Bragg peak.

2.3.2 Laue diffraction

To align the crystallographic directions of the bulk crystals, the Laue X-ray diffractometer (Photonic Science instrument), was utilized. In this method, a stationary single crystal is irradiated by means of an X-ray beam consists of a range of wavelengths (0.35 Å-2.50 Å). There is a special radiation lamp from a tungsten target used as a source of X-ray radiation. An incidental X-ray diffracts on the single crystal, and a photographic film is used to receive diffracted through the back-reflection mode-of-operation. The crystal position is

fixed for each set of planes, the parameters d_{hkl} and θ from the Eq. (2.1) are fixed. The lattice parameter d_{hkl} stands for the distance between two neighbor planes having Miller indexes h, k, l and θ is the angle formed by impinge X-ray beam. The diffractometer uses a polychromatic beam of radiation. The beam consists of an appropriate range of wavelength λ, which gives rise to the Laue spot in the reciprocal lattice in accordance with the Eq. (2.1). From the resulting diffraction pattern one can study the information about crystal structure of the sample, like crystal symmetry along with the given direction and its orientation. The pattern reveals a real symmetry of the crystal and represents the Fourier transform of the crystal lattice. Each points in reciprocal space correspond to the respective crystal systems plane having the Miller indices [111, 112]. Even the estimation of the dimensions of the unit cell is quite tedious because the exact value of λ is not known for the different sets of reflection. So, the Laue method is limited to the study of crystal orientations. The position of the Laue spots on the photographic film depends on the orientation of the crystal relative to the direction of incident beam.

2.3.3 Scanning electron microscopy (SEM)

A scanning electron microscope (SEM) is one of the most powerful and productive microscope uses electrons as a probe to images a specimen by scanning it with a beam of electrons. It allows the researchers to examine various specimens to investigate the surface morphology, average crystallite size, and the surface-related phenomenon of the sample. SEM allows the characterization and observation in a wide length scale nanometer (nm) to micrometer μm of organic and inorganic heterogeneous compounds. Its ability to obtain 3-D like images of the surfaces and large depth of field, allows large specimen to be in focus at a time, makes popular in the field of materials science and technology. It is a non-destructive technique, *i.e.*, the sample can be reused after scanning. Apart from these, the primary application of SEM is to obtain high magnification 10 – 10000X topographic images by using electrons instead of light to form an image, make the SEM much more versatile [113].

Working principle of SEM

The working principle of SEM is based on the interaction of electrons generated from the electron gun with the specimen's surface. Fig. 2.8 represents a simplified block diagram explaining the working principle and experimental set up of scanning electron microscope (SEM). At the top of Fig. 2.8, a beam of electrons is generated by an electron gun. The electron beam travels in a vacuum through the vertical path of the microscope.

The electrons beam is accelerated with dozen of KeV energy. The accelerated beam travels across the electromagnetic lenses, which is used to focus the beam down towards the sample. The condenser lenses define the size of the electron beam or resolution during the scanning coils are utilized to raster the beam onto the surface of the sample [113, 114].

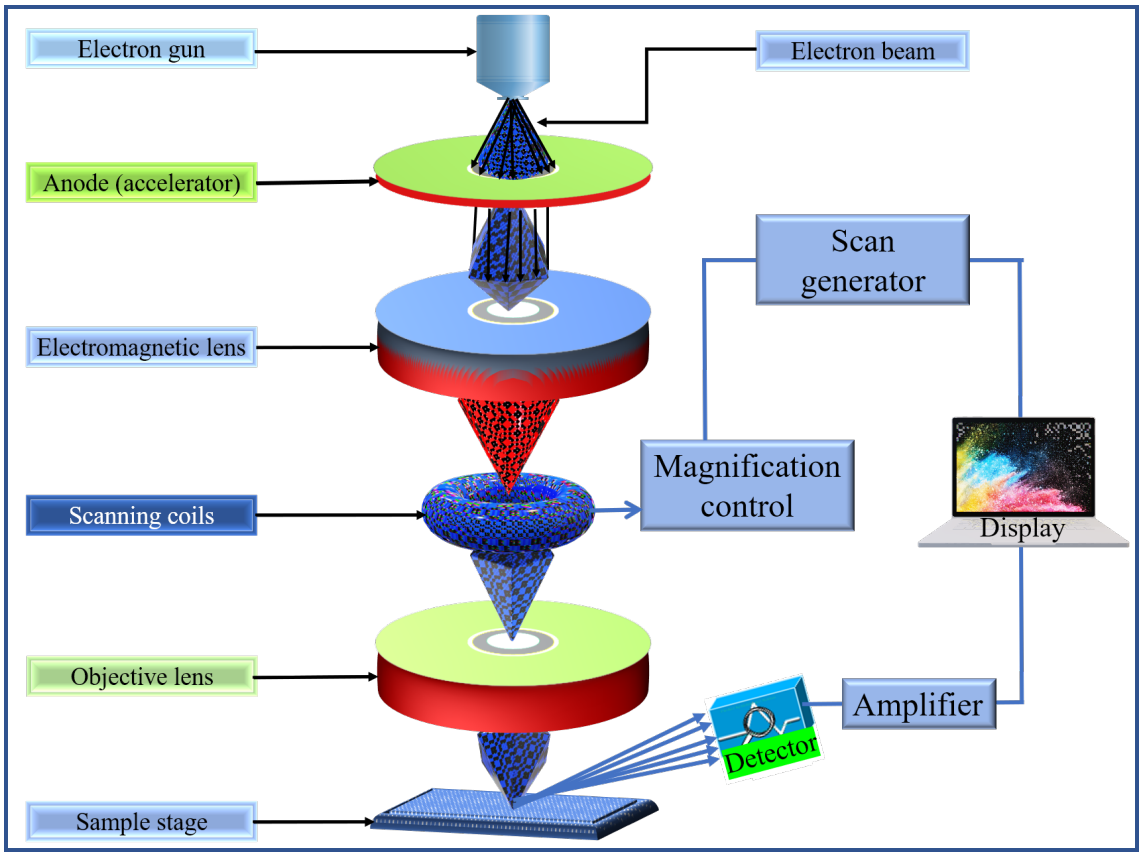

Fig. 2.8 A simplified block diagram showing the working principle of scanning electron microscope (SEM).

The objective lens is used to focus the beam and plays a crucial role in determining the final diameter of the electron probe. Once the beam strikes the sample, X-rays and electrons are ejected from the surface of sample. The detectors gather these backscattered electrons, secondary electrons and X-rays to convert them into a meaningful signal and, after amplifying, sent to a computer screen, which produces the final image. The emission of secondary electrons (Fig. 2.8 and 2.9 (a)) from the surface of specimen is confined to a region near the beam impact zone, which permits the information to be obtained at a very high resolution. The morphologic images seen on a computer provide a 3-D appearance due to the large depth of field. Sample preparation for SEM characterizations is too easy as it does not require much samples preparation activities, and the unique advantage is

specimen thickness, which is not under consideration. The surface of the sample must be clean and smoothed in order to achieve better surface morphological and grain size information before it is scanned [115].

In the SEM experiment, the area or the microvolume to be examined is irradiated with a finely and precisely focused electron beam, which is swept across the surface of the specimen to form a topographic image at a given position. The various types of signals are produced with the interaction of incident electron beam and specimen include characteristic X-rays, cathodoluminescence, backscattered electrons, auger electrons, and secondary electrons as shown in Fig. 2.9 (a). These informative signals are used to examine many characteristic features of the sample (morphology, surface topography, compositions, etc.), which is obtained from precise emission volume within the specimen. The secondary and backscattered electrons signals are of high interest for 3-D like imaging purposes because of these results primarily as differences in surface topography. The emission of secondary electrons is confined to a small area near the beam impact of certain choices of the beam energy that permits images to be observed at a resolution same as the magnitude of the size of the imping electron beam. The three-dimensional view of the images originated due to the large depth of the field and the shadowed relief effect of the backscattered and secondary electron contrast.

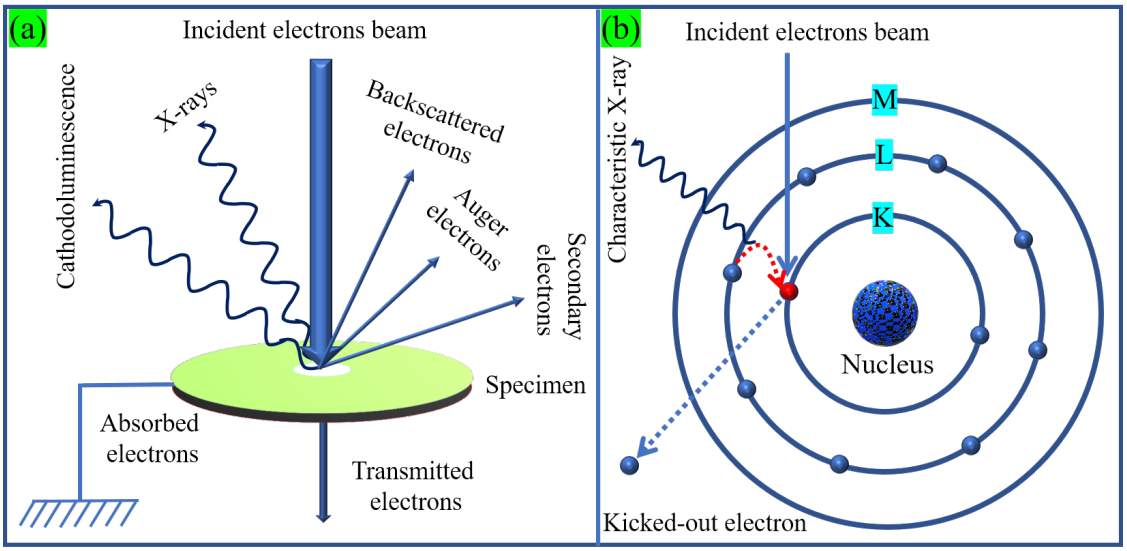

Fig. 2.9 (a) The outcomes of incident beam in the form of various signals produced from the specimen, and (b) Schematic of diagram of X-rays are generation using EDX followed by a two-step process.

With the generated characteristic X-rays as a result of electrons bombardment in SEM experiment, the analysis of X-rays radiation emitted from the specimen used to examine quantitative and qualitative elemental information from a specific region of a specimen sees the next section.

2.3.4 Energy dispersive X-ray spectroscopy (EDS or EDX)

Energy dispersive X-Ray analysis (EDAX) or Energy Dispersive X-ray Spectroscopy (EDS or EDX) is an analytic technique used together with the transmission or scanning electron microscopy (SEM) to determine the chemical composition, elemental fraction and their mapping (homogeneity) analysis of a sample, etc. EDX is a non-destructive method used to immediately calculation of all constituent elements having $Z \geq 11$. The characterization abilities (features as small as 1 μm or less can be analyzed) are due to the fundamental principle that each chemical constituent has a unique electronic structure, consequently producing X-rays of definite energy fundamental characteristic of an element allowing its chemical identification.

2.3.5 Transmission electron microscopy (TEM)

The transmission electron microscope (TEM) is a versatile and high magnification technique for probing the structure and morphology of materials. TEM is used to characterize the morphological information like shape, size, and distribution of constituents. TEM is operated in various mode of operation, depending upon the requirement users utilized this technique like HRTEM (high-resolution TEM), selected area electron diffraction along with supplementary units like EDX (electron dispersive X-ray spectroscopy) and elemental mapping [115, 116].

TEM consists of an electron gun, a vacuum system, electromagnetic lenses, a high voltage generator, recording devices, and the associated electronics. TEM uses electrons of a lower wavelength, making it possible to get a high-resolution image at the atomic length scale. A well-focused electron beam obtained from electron gun assembly and electromagnetic condenser lenses is accelerated by an anode, which is typically at 100 KeV with respect to the cathode. The beam is restricted by the condenser aperture, which stops un-collimated electrons. The collimated high energy (200 KeV and above) beam of electrons strikes the specimen and gets scattered depending upon the thickness and specimen electron transparency. Part of the scattered electron beam undergoing phase and amplitude change during scattering is transmitted, and the same is focused by the objective lens, which forms an image on a phosphor screen or charge-coupled device camera. To

block the high-angle diffracted electrons, objective apertures can be adjusted in order to enhance the contrast. The data was collected in transmission mode with limitation in sample geometry that should be very thin (less than 100 nm) [113].

Data analysis

The distributed particles of the TEM micrograph are analyzed for shape and size distribution. The histograms of particle distribution (particle size vs. the number of particles) are plotted with Image J and CrysTBox software. Fitting of the data using Lorentzian distribution provides the average particle size. The selective area electron diffraction (SAED) pattern is used to make sure phase quality and crystallinity of the samples. The diffraction pattern is indexed by calculating the inverse of its radii and matching it with interplanar spacing (d) in reciprocal space of XRD data using WinPLOTR software.

High-resolution transmission electron microscopy (HRTEM)

High-resolution transmission spectroscopy is an imaging mode of operation of the TEM that provides the high resolution micrographs of the crystallographic structure of a sample at the atomic length scale. The transmitted and scattered beams are used to create an interference image. The phase-contrast image of HRTEM can be as small as the unit cell of a crystal. It can produce images with high resolution below 0.1 Å at magnification above 50 million times. The basic alignment of TEM and sample are height, rotation center, orientation, defocus, astigmatism, etc. The voltage applied for the electron gun is nearly 200 KeV. The well-distinguished atomic planes of HRTEM are indexed by calculating the d (interplanar distance) and compared with the XRD data to confirm the phase quality at nano lenght scale [117].

2.3.6 X-ray photo electron spectroscopy

X-ray photoelectron spectroscopy (XPS) is also known as electron spectroscopy for chemical analysis (ESCA). It is a surface-sensitive spectroscopic technique widely used to investigate the chemical compositions as well as their chemical and electronic state of surfaces. XPS technique is based on the concept of photoelectric effect, was addressed in the mid-1960's by Kai Siegbahn and his research group at the University of Uppsala, Sweden. The core electrons are locally closed to the nucleus and having binding energies characteristic corresponds to element specific. The energy of these core electrons highly matched with Mg K_α and Al K_α. The concept of photon electron was used to illustrates the

ejection of electrons from a surface when X-rays (photons) were incident upon it [118, 119]. By measuring the kinetic energy of these photo electron, binding energy attributed with following Equation:

$$K.E. = h\nu - B.E. - \phi \tag{2.2}$$

where hν is energy of incident photons and ϕ is work function of specific surface.

2.3.7 X-ray absorption spectroscopy

X-ray absorption spectroscopy (XAS) is widely used to determine the local electronic states and local chemical enviourment, *i.e.*, element specific properties. This type of spectroscopy is known as inner shell spectroscopy, because X-rays are interacting core electron rather than valance electrons. For this high-energy X-rays (few KeV to MeV) are used which mostly avilable at synchrotron radiation. The core electron are excited by these synchrotron X-rays. When the energy of these X-rays are higher than the binding energy of core electron then absorption is enhanced, if K electron is excited by absorbing the energy then its known as K-edge. As the valances of element is increase the edge line is shifts to higher energy. Mostly XAS is done in two modes first one is TEY (Total electron yield) and other is TFY (Total fluorescence yield). In fluorescence mode incident energy is fixed and energy dependence of secondary photon is measured [120–122].

2.3.8 X-ray magnetic linear dichroism (XMLD)

X-ray magnetic linear dichroism (XMLD) has been providing detailed information about the magnetic and electronic structure of specimen at the molecular level. The definition of dichroism is the polarization dependence of light absorption by a material. It occurs when the symmetry of the material is broken. XMLD is obtained by the difference between linear and vertical XAS spectra. It used to study the phenomena of exchange biasing and anisotropy. Ideally, the magnetic anisotropy needs to be measured by rotating the orientation of the magnetization. By the sum rule for linear dichroism relates the anisotropic part of spin-orbit interaction and the integrated intensity to the charge quadrupole moment [120–123].

2.3.9 Neutron diffraction

Apart from the electron and X-ray diffraction, neutrons exhibit the neutral charge, the mass of 1.0087 atomic mass unit (amu), half $(\frac{1}{2})$ spin and magnetic moment of -1.9132 μ_N

(nuclear magneton). The respective properties make neutrons an effective tool for materials physicists. Cold and thermal neutrons have a total energy of about one meV (0.1 - 10 meV) and 25 meV (5 - 100 meV), respectively, which correspond to the wavelength of about 9.0 Å and 1.8 Å , respectively. Therefore, providing an ideal probe for the study of magnetic and structural features in microscopic and mesoscopic length scales [124].

The small-angle neutron scattering (SANS) is a versatile technique in order to study structural and magnetic properties of specimens on mesoscopic length scale, covering 10 to 1000 Å [125]. In the case of the neutron scattering experiment, the intensity is measured of the scattered monochromatic neutrons as a function of scattering angle by the specimen under the investigation, with the aim to determine the scattering cross-section as a function of propagation wave vector, which is given by:

$$Q = \frac{4\pi}{\lambda} \sin(\theta) \tag{2.3}$$

where, 2θ is the angle of scattering and λ wavelength of monochromatic neutron beam.

2.3.10 Magnetic property measurement system (MPMS)

Magnetic property measurement system (MPMS) is an advanced technique used for the sensitive and effective measurements of the magnetic moments of small samples (powder, single crystals, thin films, pallets, etc.) over a broad range of temperatures and magnetic fields at various frequencies, choice made depending upon the requirements. Superconducting Quantum Interference Device (SQUID) is a very sensitive magnetometer widely used for the same. Working principle of SQUID magnetometer is based on the tunneling effect of Cooper pairs across a Josephson junction of two superconductors separated by an insulating gap [126]. The key element of SQUID is a superconducting ring with two Josephson Junctions.

dc magnetization

In dc magnetic measurements, the sample is magnetized by a constant value of the applied magnetic field to determine the equilibrium value of the magnetic moment in a sample. The moment is measured by induction or torque techniques, where the sample moment is constant during the measurement time. dc magnetometry is one of the most straight forward and versatile technique of measuring the magnetization (**M**) of magnetic materials. By measurement of magnetic flux density (B) as a function of magnetic field strength (H) provides M as $B = \mu_0(H+M)$. dc magnetic susceptibility χ_{dc} measures the change in

magnetization with respect to an applied magnetic field strength by $M = \chi(H)$, valid only in the paramagnetic phase, although sometimes used in the magnetically ordered phase when using low value of field and where a linear regime is observed. As a matter of fact, ordering into the antiferromagnetic state from a paramagnetic state is usually convoyed by a peak and a reduction in susceptibility appears on decreasing the temperature. In the paramagnetic phase of materials, the temperature dependence of the magnetic susceptibility (χ) is given by the widely known Curie-Weiss law:

$$\chi = \frac{C}{T - \theta_P} \tag{2.4}$$

where C is Curie constant corresponds to materials and T is the absolute temperature in kelvins. θ_P is the Curie-Weiss temperature related to the exchange interaction between magnetic moments, and θ_P will be positive for FM ordering, zero for purely paramagnetic materials, and negative for AFM order.

The experimental χ^{-1} vs. T ($\chi^{-1}(T)$) of materials often presents a curvature that cannot be simply elucidated by a Curie-Weiss law. This discrepancy was fixed by means of Modified Curie-Weiss (MCW) law to elucidate the chi in the paramagnetic regimes [127], according to formula as shown in Equation.

$$\chi = \chi_0^* + \frac{C^*}{T - \theta_P} \tag{2.5}$$

where θ_P represents the paramagnetic Curie temperature and C^* the Curie constant. This formula also involves the temperature-independent term χ_0^* [128, 129]. The temperature independent quantity χ_0^* indicate that care must be taken in attributing μ_{eff}^* deduced from C^*, *i.e.*, $\mu_{eff}^* \sim \sqrt{8C^*}$ when units are used in a molar.

dc magnetic susceptibility (χ_{dc}) and the necessary magnetization measurement results attached in this thesis were performed using a SQUID magnetometer (Quantum design). The temperature range of the SQUID varied from 2 K up to 350 K, and the dc magnetic field B can be spans up to 7 T with this setup, and collected the data in the interesting range of filed and temperature depending upon the requirements. Fixing a constant field and varying the temperature, the temperature dependence of χ_{dc} can be mapped. At a constant temperature and varying the field strength yields the bulk magnetization, *i.e.*, isothermal magnetization curves (M vs. H curves or M(H)) were also obtained. In this case, data were collected while decreasing the applied magnetic field in the range of $\pm$ 7 T.

In order to obtain the sample's magnetic parameters like Curie (T_C), Neel (T_N) temperature, the low field magnetization measurements were performed. For this purpose, the temperature dependence of magnetization at low fields is acquired after the sample

cooled without applied magnetic field (called ZFC protocol) and/or with field cooled (FC protocol), the details given below:

• **Zero field cooling (ZFC):** the sample is cooled with H = 0 Oe to the lowest required temperature, thereafter the magnetic field is applied in a fixed orientation of sample and the consequent magnetization measurements are made while sweeping the temperature in a variable range of temperatures that one can measure from 2 K up to 390 K) with this setup.

• **Field cooling (FC):** the sample is cooled in the presence of the required value of applied magnetic field to the desired temperature, thereafter the data is collected during the warming up to the desired value of temperature with a constant applied field (called FCW). Sometimes, it is preferred to perform the measurements while cooling in the presence of an applied magnetic field, this type of measurement is called FCC.

ac magnetization

ac magnetic measurements, in which an ac drive magnetic field is superimposed on the dc field, and the resulting ac moment is measured of the sample. The resulting sample moment is time-dependent, yielding information of magnetization dynamics makes an important tool for characterization of many magnetic materials which are missing in dc magnetometry, where the sample moment is constant throughout the measurement time.

ac susceptibility χ_{ac} is similar to χ_{dc} in many aspects at very low frequencies. The frequency dependency provides additional information about the magnetic nature of the sample. At higher frequencies, the ac moment of the sample does not follow the dc magnetization curve due to dynamic effects in the sample. For this, the χ_{ac} is often known as the dynamic susceptibility. In this case, the χ_{ac} measurement yields two distinct quantities and defined as

$$\chi_{ac} = \chi' - i\chi'' = \sqrt{(\chi')^2 + (\chi'')^2} \tag{2.6}$$

$$\textit{where} \quad \chi' = \chi\cos(\phi); \quad \chi'' = \chi\sin(\phi) \quad \textit{and} \quad \phi = \arctan\left(\chi''/\chi'\right) \tag{2.7}$$

where the ϕ is the phase shift (relative to the driver signal), χ' is the real part (or in-phase), and component χ'' is the imaginary part (or an out-of-phase) of the χ [130].